Quantitative study of multiphoton multiple ionization: Second-harmonic Nd:YAG laser ionization of the doubly excited $2p^2\,{}^3P$ bound state of H^-

Theodoros Mercouris and Cleanthes A. Nicolaides

Theoretical and Physical Chemistry Institute, National Hellenic Research Foundation,
48 Vasileos Constantinou Avenue, 116 35 Athens, Greece

Starting with the H^- $2p^2\,{}^3P$ excited bound state, we have studied the problem of direct versus sequential two-photon, two-electron ionization with linearly polarized laser light of $\lambda = 5320$ Å and intensity $I = 1.4 \times 10^9$ W/cm². The theory is nonperturbative and electronic-structure oriented. It allows for the multiconfigurational zero-order representation of bound and autoionizing states, for electron correlation, and for the effects of nonorthonormality which cause multielectron excitation even without correlation corrections. The one- and two-electron multichannel continua are represented by square-integrable complex exponential functions. The results show that the sequential process is dominant, even though there exists the H^- $4s4p\,{}^3P^o$ autoionizing state, which is near resonance. However, the direct process would dominate if the autoionization width, which is computed to be 1.16×10^{-3} a.u., happened to be smaller by about a factor of 100, which is a realistic possibility for other systems.

PACS number(s): 32.80.Rm, 32.80.Fb, 32.80.Wr, 32.80.Dz

I. INTRODUCTION

It is of fundamental importance to have a quantitative understanding of the interplay between the dynamics of monophotonic or polyphotonic absorption by atoms and molecules and the characteristics of electronic structure and spectra. In this connection, strong interest has developed in studying and interpreting the formation of multiply charged ions upon laser irradiation of atoms [1–8], a phenomenon which has given rise to the question of the character of the related physical processes ("mechanism") involved [1–15]: To what extent is it sequential (S) or direct (D) ionization? S ionization implies that the creation of the final multiply charged ion A^{+q} (q is the total charge) goes through the stepwise formation of the intermediate ions,

$$A^{+1}, A^{+2}, \ldots, A^{+(q-1)},$$

whereas D ionization involves the simultaneous excitation and ionization of q electrons with the possible assistance of multiply excited states (MES).

From the point of view of *ab initio* theory, the study of the above problem must necessarily take into account the specifics of the system "atomic state plus laser." The plurality of such systems implies that in order to draw reliable conclusions on this phenomenon, extensive quantitative information is needed. A theoretical research program for obtaining such information must pay respect to the spectral features of each system of interest and must implement advanced computational methods which can quantify efficiently interelectronic interactions and real and virtual transition processes to all orders.

In this paper we apply our previously published many-electron many-photon theory (MEMPT) for the treatment of multiphoton ionization in polyelectronic systems [16–18] and of MES [19-21] to the two-photon ionization

($\lambda = 532$ nm, second harmonic of Nd: YAG) of the H^- $2p^2\,{}^3P$ bound state. This theory is nonperturbative and therefore applicable to the weak-field as well as to strong-field case. In the present application, an extension has been made in order to allow the calculation of double-ionization rates by incorporating a square-integrable representation of the double continuum (see Sec. II B). The preparation scheme of the H^- $2p^2\,{}^3P$ bound state is shown in Fig. 1 [17]. This state decays via
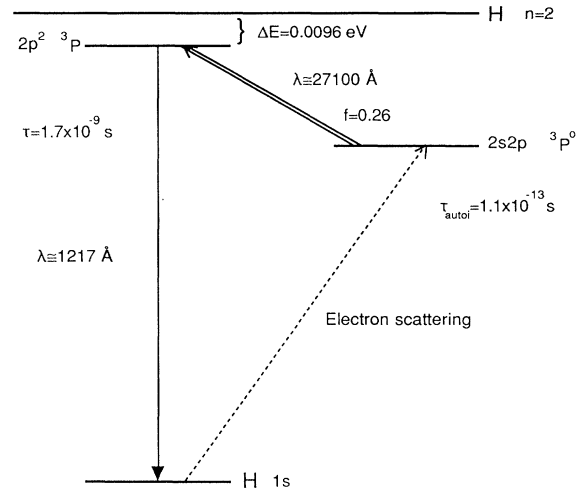

FIG. 1. The H^- states of interest with their intrinsic properties, energy, and lifetime, before the application of the laser. The numbers are taken from Ref. [17]. Upon preparation in a scattering experiment [24] of the H^- $2s2p\,{}^3P^o$ autoionizing state, the $2p^2\,{}^3P$ bound state is reached via one-photon absorption of $\lambda \approx 27\,100$ Å. The oscillator strength is $f = 0.26$. The ${}^3P$ state can then be observed via a continuum of photon and electron emission, whose rate rises by orders of magnitude around $\lambda \approx 1217$ Å [22].

a one-photon, two-electron transition process into the H $1s\epsilon p$ $^3P^\circ$ continuum, with a lifetime of 1.7×10^{-9} s. The distribution of this emission rate is such that the transition occurs essentially around $\lambda\approx1217$ Å [22].

Compared to the case of the closed-shell He $1s^2$ ^1S ground state, which was investigated in previous studies of double ionization using the weak-field perturbation theory approximation [10,13], starting the excitation scheme from H^- $2p^2$ ^3P has meaningful advantages: This state is close to the first- and second-ionization thresholds and the strength of Coulomb interactions is weak. Hence, one may employ the Nd:YAG second harmonic at $\lambda=5320$ Å, under controllable intensity conditions, in order to strip H^- of its two electrons with only two photons. Furthermore, the opportunity is given to examine the importance of intermediate MES explicitly: Inside the first-ionization continuum, we have computed that there exists the quasibound resonance H^- "$4s4p$" $^3P^\circ$, which matches the one-photon frequency, thereby increasing the probability for direct ionization.

II. COMPUTATIONAL METHOD

A. Calculation of the field-free wave functions, energies, and widths

The doubly excited states involved in the proposed excitation scheme (see Fig. 2) were calculated according to the state-specific theory of MES [19–21]. The wave function of H^- $2p^2$ ^3P was computed at the multiconfigurational Hartree-Fock (MCHF) level:

$$\Psi_0=c_12p^2+c_23p^2+c_33d^2+c_44f^2 ,\qquad(1a)$$

where

$$c_1=0.93,\quad c_2=-0.34,\quad c_3=0.13,\quad c_4=0.01 .$$

Its energy,

$$E_0=-0.125\,318\,7 \text{ a.u. },$$

corresponds to an electron affinity of 0.009 eV with respect to the H $n=2$ threshold. Similarly, the MCHF wave function of the autoionizing state H^- $4s4p$ $^3P^\circ$ was obtained as

$$\Psi_0=a_14s4p+a_24p4d+a_34d4f ,\qquad(1b)$$

where $a_1=0.81, a_2=0.56, a_3=0.17$, and

$$E_0=-0.039\,523 \text{ a.u.}$$

The $4s4p$ $^3P^\circ$ state decays nonradiatively into the channels shown in Fig. 3. The partial widths were calculated by the method described in Refs. [20,21] and are included in Fig. 3. The corresponding total width was computed to be

$$\Gamma_{aut}=1.16\times10^{-3} \text{ a.u. },\qquad(2)$$

in good agreement with the results of Ho and Callaway's large calculations [23] (1.02 a.u.).
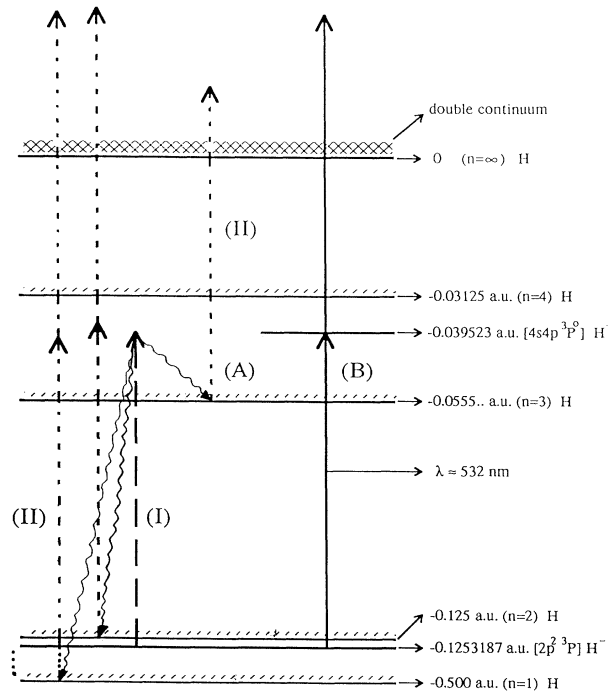
FIG. 2. The energy diagram of the states of H^- involved in the proposed interaction scheme: (A): Sequential mechanism for double ionization. The sequential mechanism consists of two independent steps. The first (I), which is marked by the arrow with the long dashes, is the single-electron photoionization of the H^- $2p^2$ ^3P bound state, leaving the neutral H in excited states. The wavy arrows indicate that at the end of the first step (I), the neutral H is in the states with principal quantum numbers $n=1,2,3$. The second step (II), which is marked by the arrows with the short dashes, consists of the photoionization of the neutral H states $n=1,2,3$. (B) Direct mechanism for double ionization. The direct mechanism, marked with the solid line arrows, couples, through the laser field of wavelength $\lambda\approx532$ nm, the initial bound state $2p^2$ ^3P with the double excited autoionizing state $4s4p$ $^3P^\circ$. Double ionization occurs by absorption of a second photon by the $4s4p$ $^3P^\circ$ autoionizing state.

FIG. 3. Continuum channels into which the $4s4p$ $^3P^\circ$ autoionizing state decays. The numbers in parentheses give the partial widths of the corresponding channels as a percentage of the total width $\Gamma_{aut}=1.16\times10^{-3}$ a.u.

B. Calculation of the direct-double-ionization rate of the H$^-$ $2p^2\,^3P$ bound state

As shown in Fig. 2 [process (B)], the direct-ionization mechanism for H$^-$ $2p^2\,^3P$-goes through the autoionizing state $4s4p\,^3P°$. This process can be written schematically as

$$2p^2\,^3P \longrightarrow 4s4p\,^3P° \longrightarrow \left\{ \begin{array}{l} \left.\begin{array}{l} \epsilon p\epsilon'p \\ \epsilon d\epsilon'd \end{array}\right\}\,^3P \\ \left.\begin{array}{l} \epsilon p\epsilon'p \\ \epsilon d\epsilon'd \\ \epsilon p\epsilon'f \\ \epsilon s\epsilon d \end{array}\right\}\,^3D \end{array}\right. \qquad (3)$$
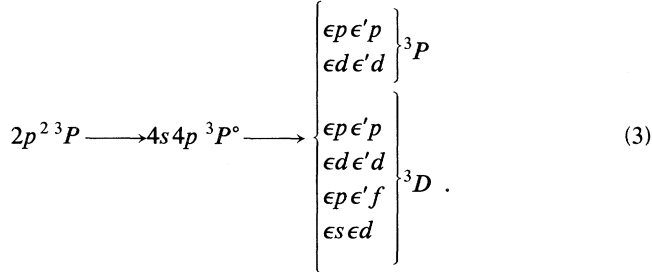
The probability for process (3) was computed in two steps: First, we allowed the coupling of $4s4p\,^3P°$ to the double continuum states and calculated the corresponding width. The orbitals of the double continuum states, $\epsilon l\epsilon'l'$, were chosen as linear combinations of complex orbitals [18]:

$$\epsilon l \approx \rho^{n+1}e^{-\alpha\rho}, \quad \rho=re^{-i\vartheta}, \quad 0\leq\vartheta\leq\pi/2, \quad n=0,1,\ldots, \qquad (4)$$

$$\Gamma_D(2p^2\,^3P)=[\Gamma_D(4s4p\,^3P°)/\Gamma_{\text{total}}(4s4p\,^3P°)]\Gamma_{\text{total}}(2p^2\,^3P) . \qquad (5a)$$

In Table I we give the widths of $2p^2\,^3P$ as a function of laser frequency ω.

C. Calculation of the rates of the independent steps of the sequential double ionization of H$^-$ $2p^2\,^3P$

The sequential mechanism involves two independent excitation steps (see Fig. 2, processes A I and A II). The first step (Fig. 2 A I) is simply the single-electron photoionization of the H$^-$ $2p^2\,^3P$ bound state, leaving the neutral H in a number of bound states. This is schematically shown in Fig. 4. The partial widths of the single-electron photoionization of the H$^-$ $2p^2\,^3P$ bound state to the various ionization channels (see Fig. 4) add to a total photoionization rate for field intensity $I=1.4\times10^9$ W/cm^2 of

$$\Gamma_I=1.5\times10^{-6}\text{ a.u.} \qquad (6)$$

In addition, the rate of Eq. (6) is proportional to field intensity I,

$$\Gamma_I\sim I . \qquad (6a)$$

Part of the stepwise path is the possibility of creating excited states of H through the autoionization of the double excited state $4s4p\,^3P°$. However, this is not taken into account, because the rate for this path, for wavelengths around 532 nm, is of the order of 10^{-10} a.u. (see Table I),

which were kept orthogonal to the bound hydrogen orbitals up to principal quantum number $n=4$. For example, the $\epsilon s\,L^2$ orbital was kept orthogonal to the 1s, 2s, 3s, and 4s hydrogenic orbitals. By computing the complex energy of the total Hamiltonian matrix as a function of ϑ and α [the parameters of the basis set, Eq. (4)], we obtained the stabilized width

$$\Gamma_D(4s4p\,^3P°)=0.3\times10^{-6}\text{ a.u.}=(2.6\times10^{-4})\Gamma_{\text{aut}} \qquad (5)$$

for field intensity $I=1.4\times10^9$ W/cm^2 and laser field wavelength around 532 nm ($\omega\cong0.0858$ a.u.).

Note that electron correlation in the doubly ionized state is taken into account through the calculation of matrix elements of the type

$$\langle\epsilon_1l_1\epsilon_2l_2|H|\epsilon_3l_3\epsilon_4l_4\rangle ,$$

and that the nonorthonormality among the state-specific orbitals which are computed in their own self-consistent field is included whenever it arises [16,19].

Next, we computed the width of the $2p^2\,^3P$ state which results from the coupling to the double continuum via the $4s4p\,^3P°$ state. In doing so, we have to incorporate the previously computed rates for autoionization and for direct-double-electron ionization of the $4s4p\,^3P°$ state by assuming the same ratio as that of Eq. (5). Thus, we write

which is four orders of magnitude smaller than the corresponding rate through pure single-electron photoionization [see Eq. (6)].

The second step (Fig. 2, A II) is the photoionization of

TABLE I. Total width in a.u. of $2p^2\,^3P$ of H$^-$. The width of $2p^2\,^3P$ which is due to the direct coupling with the double continuum, Γ_D, was calculated from the equation

$$\Gamma_D(2p^2\,^3P)=[\Gamma_D(4s4p\,^3P°)/\Gamma_{\text{total}}(4s4p\,^3P°)]\Gamma_{\text{total}}(2p^2\,^3P)$$

with $\Gamma_{\text{total}}(4s4p\,^3P°)\approx\Gamma_{\text{aut}}=1.16\times10^{-3}$ a.u. and field intensity $I=1.4\times10^9$ w/cm^2.

ω (a.u.)	$\Gamma_{\text{total}}(2p^2\,^3P)$ (a.u.)	$\Gamma_D(2p^2\,^3P)$ (a.u.)
0.080 00	8.2[−12]	2.1[−15]
0.081 00	1.2[−11]	3.1[−15]
0.082 00	1.9[−11]	4.9[−15]
0.083 00	3.4[−11]	8.8[−15]
0.084 00	7.8[−11]	2.0[−14]
0.085 00	2.8[−10]	7.3[−14]
0.085 50	6.6[−10]	1.7[−13]
0.085 80	8.2[−10]	2.1[−13]
0.086 00	7.4[−10]	1.9[−13]
0.088 00	5.4[−11]	1.4[−14]
0.089 00	2.6[−11]	6.8[−15]
0.090 00	1.5[−11]	4.0[−15]

I

$2p^2\,{}^3P$ $\xrightarrow{\;\hbar\omega\;}$

$1S_H\ \varepsilon p$ ${}^3P^o$ (0%)

$2S_H\ \varepsilon p$ (0%)

$2P_H\ \varepsilon s$ ${}^3P^o$ (17%)

$2P_H\ \varepsilon d$ (3%)

$3S_H\ \varepsilon p$ (0%)

$3P_H\ \varepsilon s$ ${}^3P^o$ (2%)

$3P_H\ \varepsilon d$ (7%) $\Gamma_I = 1.54\times10^{-6}$ a.u.

$3d_H\ \varepsilon p$ (35%)

$3P_H\ \varepsilon d$ (12%)

$3d_H\ \varepsilon p$ ${}^3D^o$ (24%)

FIG. 4. First step of the sequential mechanism. Continuum channels which are coupled through the laser field to the H^- $2p^2\,{}^3P$ bound state. The numbers in parentheses give the partial widths of the corresponding photoionization channels as a percentage of the total width.

II

$2P_H$

m = −1 (2.4%) $\Gamma_{-1} = 0.23\times10^{-10}$ a.u.

m = 0 (1.2%) $\xrightarrow{\;\hbar\omega\;}\varepsilon l$ $\Gamma_0 = 0.22\times10^{-10}$ a.u.

m = 1 (19.4%) $\Gamma_1 = 0.23\times10^{-10}$ a.u.

$3P_H$

m = −1 (8.1%) $\Gamma_{-1} = 0.46\times10^{-6}$ a.u.

m = 0 (4.1%) $\xrightarrow{\;\hbar\omega\;}\varepsilon l$ $\Gamma_0 = 0.53\times10^{-6}$ a.u.

m = 1 (6.6%) $\Gamma_1 = 0.46\times10^{-6}$ a.u.

$3d_H$

m = 2 (29%) $\Gamma_2 = 0.23\times10^{-6}$ a.u.

m = 1 (14.5%) $\xrightarrow{\;\hbar\omega\;}\varepsilon l$ $\Gamma_1 = 0.24\times10^{-6}$ a.u.

m = 0 (16.0%) $\Gamma_0 = 0.28\times10^{-6}$ a.u.

$\Gamma_{II} = 4.7\times10^{-7}$ a.u.

FIG. 5. Second step of the sequential mechanism. Neutral H bound-state photoionization rates (in a.u.) due to a laser field of intensity $I = 1.4\times10^9$ W/cm^2 and frequency 0.0858 a.u. (≈ 532 nm). The numbers in parentheses give the percentage of the participation of the corresponding state to the total population of the bound states.

neutral H bound states, produced after the first step. Figure 5 shows the second step of the S mechanism with details concerning the population distribution of the neutral H bound states, characterized by the angular momentum quantum number l and the z component of the angular momentum $l_z = m$. We note here that we assume that our initial state $2p^2\,{}^3P$ has been prepared with the z component of its total angular momentum equal to 1. Thus, the final states of the first step (Fig. 2, A I and Fig. 4) have the same z component of their total angular momentum as the initial $2p^2\,{}^3P$ state. The result of this m-dependent excitation is that the population of the H states at the end of the first step of the sequential mechanism depends on m (see Fig. 5). The calculated photoionization rates for the different bound states (Fig. 5) add to a total rate for $I = 1.4\times10^9$ W/cm^2 of

$$\Gamma_{II} = 4.7\times10^{-7}\ \text{a.u.} \tag{7}$$

This rate is also proportional to field intensity I,

$$\Gamma_{II} \sim I \ . \tag{7a}$$

Since the S mechanism is a combination of two independent steps, we can say that the number of H^+ ions produced through this mechanism $(N_{2,S})$ is proportional to the product Γ_S of the two rates of Eqs. (6) and (7) (see Sec. III and Ref. [10]), i.e.,

$$N_{2,S} \sim \Gamma_S = \Gamma_I \Gamma_{II} = 7.1\times10^{-13}\ . \tag{8}$$

At the same time, using (6a) and (7a),

$$\Gamma_S \sim I^2\ . \tag{8a}$$

III. RESULTS

Following the approach of Refs. [3,10] for the dynamics of the ionization process, we write the rate equations

$$
\begin{aligned}
\dot{N}_0(t) &= -(\Gamma_I + \Gamma_D)N_0(t), \\
\dot{N}_1(t) &= \Gamma_I N_0(t) - \Gamma_{II} N_1(t) \quad \text{or} \\
\dot{N}_2(t) &= \Gamma_D N_0(t) + \Gamma_{II} N_1(t)
\end{aligned}
\qquad
\begin{bmatrix} \dot{N}_0(t) \\ \dot{N}_1(t) \\ \dot{N}_2(t) \end{bmatrix}
=
\begin{bmatrix} -(\Gamma_I+\Gamma_D) & 0 & 0 \\ \Gamma_I & -\Gamma_{II} & 0 \\ \Gamma_D & \Gamma_{II} & 0 \end{bmatrix}
\begin{bmatrix} N_0(t) \\ N_1(t) \\ N_2(t) \end{bmatrix},
\tag{9}
$$

where N_0, N_1, and N_2 are the number of H^- atoms, H atoms, and H^+ atoms, respectively.

Assuming that the rates in Eqs. (9) are independent of time (or that the laser field intensity is independent of time) and expanding $N_0(t)$, $N_1(t)$, and $N_2(t)$ in series,

$$
\begin{bmatrix} N_0(t) \\ N_1(t) \\ N_2(t) \end{bmatrix}
= \sum_{n=0}^{\infty}
\begin{bmatrix} C_{0n} \\ C_{1n} \\ C_{2n} \end{bmatrix}
t^n, \quad C_{00}=1,\ C_{10}=C_{20}=0
\tag{10}
$$

we can write the system of differential equations (9) in the form

$$
\sum_{n=0}^{\infty} (n+1)
\begin{bmatrix} C_{0n+1} \\ C_{1n+1} \\ C_{2n+1} \end{bmatrix}
t^n
$$

$$
= \sum_{n=0}^{\infty}
\begin{bmatrix} -(\Gamma_I+\Gamma_D) & 0 & 0 \\ \Gamma_I & -\Gamma_{II} & 0 \\ \Gamma_D & \Gamma_{II} & 0 \end{bmatrix}
\begin{bmatrix} C_{0n} \\ C_{1n} \\ C_{2n} \end{bmatrix}
t^n, \tag{11a}
$$

or, equivalently,

$$
\begin{bmatrix} C_{0n+1} \\ C_{1n+1} \\ C_{2n+1} \end{bmatrix} = \frac{1}{n+1} \begin{bmatrix} -(\Gamma_{I}+\Gamma_{D}) & 0 & 0 \\ \Gamma_{I} & -\Gamma_{II} & 0 \\ \Gamma_{D} & \Gamma_{II} & 0 \end{bmatrix} \begin{bmatrix} C_{0n} \\ C_{1n} \\ C_{2n} \end{bmatrix} ,
$$

$$ n = 0, 1, \dots . \quad (11b) $$

Then, by combining Eqs. (10) and (11), we obtain for $N_2(t)$:

$$
N_2(t) = 0 \times t^0 + \Gamma_D t^1
$$
$$
+ \tfrac{1}{2}[\Gamma_I \Gamma_{II} - \Gamma_D(\Gamma_I+\Gamma_D)]t^2 + \cdots . \quad (12)
$$

For short interaction time, Eq. (12) shows that we can distinguish the number $N_{2,S}$ of the H^+ atoms corresponding to the S mechanism from the number $N_{2,D}$ of H^+ atoms corresponding to the D mechanism:

$$
N_{2,S} \cong \tfrac{1}{2}\Gamma_I \Gamma_{II} t^2
$$
$$
= \tfrac{1}{2}\Gamma_S t^2 \quad \text{through Eq. (8) ,} \quad (13a)
$$

$$
N_{2,D} = \Gamma_D t . \quad (13b)
$$

From Eqs. (13a) and (13b) we see that for times greater than

$$
\tau = \frac{2\Gamma_D}{\Gamma_S} , \quad (13c)
$$

the S mechanism for the production of H^+ atoms dominates. Using Table I and Eqs. (12) and (13), this lower bound is about 1 a.u. (2.4×10^{-17} s).

IV. SYNOPSIS AND CONCLUSIONS

We presented a method for dealing with the problem of multiphoton, multielectron excitation of real atomic spectra. The theory is applicable to weak fields, as in the present case, as well as to strong ones. Electron correlation is included in the initial (ground or excited, closed-shell or open-shell state), in the intermediate, and in the final states of the two-electron multichannel continuum by using function spaces which are state specific. Furthermore, the physically important reorganization of the self-consistent field as the excitation "travels" through the spectrum is included explicitly via the computation of nonorthonormality effects [16,19].

The system "H^- $2p^2 {}^3P$ plus second harmonic Nd:YAG" chosen for this work presents a realistic as well as prototypical situation for investigating the possibility of enhancement of the probability of the direct multiphonon multiple-ionization process. Our theory and computations lead to the conclusion that the S mechanism dominates for times longer than 1 a.u.

Yet, it is worth pointing out the following: For laser field intensities of the order of 10^9 W/cm^2 and for wavelengths around 532 nm, in the rotating-wave approximation we obtain for Γ_D $(2p^2 {}^3P)$ (see also Table I):

$$
\Gamma_D(2p^2 {}^3P) = \Gamma_{\text{total}}(2p^2 {}^3P) \frac{\Gamma_D(4s4p\ {}^3P^{\circ})}{\Gamma_{\text{aut}}(4s4p\ {}^3P^{\circ})}
$$
$$
\approx \left[\frac{V^2}{\Gamma_{\text{aut}}}I\right]\frac{I}{\Gamma_{\text{aut}}} \approx \left[\frac{V}{\Gamma_{\text{aut}}}\right]^2 I^2 , \quad (14)
$$

with

$$
V = \langle 2p^2 {}^3P |z| 4s4p\ {}^3P^{\circ} \rangle \cong 4.89 \times 10^{-3} . \quad (14a)
$$

Thus, it follows that the time τ [see Eq. (13c)] determining the moment after which the S mechanism dominates is

$$
\tau \approx \left[\frac{V}{\Gamma_{\text{aut}}}\right]^2 . \quad (15)
$$

Equation (15) implies that the intermediate MES plays a crucial role through the ratio of two characteristics: The dipole matrix element with the lower state and the intrinsic autoionization width. For example, if the H^- $4s4p\ {}^3P^{\circ}$ width were a factor of 100 smaller, the direct mechanism would be significant for times appreciably larger than 1 a.u. It should not be excluded that such a situation occurs in other systems.

On the other hand, for intensities larger than 10^9 W/cm^2 but still low enough that the system is still described in terms of the same states, the total as well as the direct widths of the H^- $2p^2 {}^3P$ tend to a constant. Then, with the help of Eq. (14), the time τ goes as

$$
\tau \approx \frac{1}{I^2} , \quad (16)
$$

and the S mechanism dominates independently of electronic-structure characteristics.

[1] I. P. Zapesochnyi and V. V. Suran, Pis'ma Zh. Tekh. Fiz. **1**, 973 (1975) [Sov. Tech. Phys. Lett. **1**, 420 (1975)]; I Aleksakhin, P. Zapesochnyi, and V. V. Suran, Pis'ma Zh. Eskp. Teor. Fiz. **26**, 14 (1977) [JETP Lett. **26**, 11 (1977)].

[2] D. Felmann and K. H. Welge, J. Phys. B **15**, 1651 (1982); D. Feldmann, J. Krautwald, S. L. Chin, A. VanHellfeld, and K. H. Welge, ibid. **15**, 1663 (1982).

[3] A. L'Huillier, L. A. Lompre, G. Mainfray, and C. Manus, Phys. Rev. Lett. **48**, 1814 (1982); Phys. Rev. A **27**, 2503 (1983).

[4] G. Petite and P. Agostini, J. Phys. (Paris) **47**, 795 (1986); P. Agostini and G. Petite, Phys. Rev. A **32**, 3800 (1985).

[5] T. S. Luk, H. Pummer, K. Boyer, M. Shakidi, H. Egger, and C. K. Rhodes, Phys. Rev. Lett. **51**, 110 (1983); T. S. Luk, U. Johann, H. Egger, H. Pummer, and C. K. Rhodes, Phys. Rev. A **32**, 21 (1985).

[6] I. I. Bondar, M. I. Dudich, and V. V. Suran, Zh. Eksp. Teor. Fiz. **90**, 1952 (1986) [Sov. Phys. JETP **63**, 1142 (1986)].

[7] P. Camus, M. Kompitsas, S. Cohen, C. A. Nicolaides, M.

Aymar, M. Crance, and P. Pillet, J. Phys. B **22**, 445 (1989).

[8] A. L'Huillier, Comments At. Mol. Phys. **18**, 289 (1986).

[9] P. Lambropoulos, Phys. Rev. Lett. **55**, 2141 (1985); S. Geltman, *ibid*. **54**, 1909 (1985); K. Boyer and C. K. Rhodes, *ibid*. **54**, 1490 (1985).

[10] M. Crance and M. Aymar, J. Phys. (Paris) **46**, 1887 (1985).

[11] Xing-Dong Mu, T. Aberg, A. Blomberg, and B. Crasemann, Phys. Rev. Lett. **56**, 1909 (1986).

[12] A. L'Huillier and G. Wendin, Phys. Rev. A **36**, 5632 (1987).

[13] X. Tang and P. Lambropoulos, Phys. Rev. Lett. **58**, 108 (1987); H. Bachau and P. Lambropoulos, Z. Phys. D **11**, 37 (1989); Phys. Rev. A **44**, R9 (1991).

[14] P. Lambropoulos, Comments At. Mol. Phys. **20**, 199 (1987).

[15] K. Burnett, J. Phys. B **21**, 3083 (1988); J. Mol. Opt. **36**, 925 (1989).

[16] C. A. Nicolaides and Th. Mercouris, in *Atoms in Strong Fields,* edited by C. A. Nicolaides, C. W. Clark, and M. H. Nayfeh (Plenum, New York, 1990), p. 353.

[17] Th. Mercouris and C. A. Nicolaides, J. Phys. B **24**, L557 (1991).

[18] Th. Mercouris and C. A. Nicolaides, J. Phys. B **23**, 2037 (1990); Phys. Rev. A **45**, 2116 (1992).

[19] C. A. Nicolaides, Y. Komninos, M. Chrysos, and G. Aspromallis, in *Atoms in Strong Fields,* edited by C. A. Nicolaides, C. W. Clark, and M. H. Nayfeh (Plenum, New York, 1990), p. 493.

[20] C. A. Nicolaides, M. Chrysos, and Y. Komninos, Phys. Rev. A **39**, 1523 (1989).

[21] C. A. Nicolaides and Th. Mercouris, Phys. Rev. A **32**, 3247 (1985); M. Chrysos, Y. Komninos, Th. Mercouris, and C. A. Nicolaides, *ibid*. **42**, 2634 (1990).

[22] C. W. Drake, Astrophys. J. **184**, 145 (1973).

[23] Y. K. Ho and J. Callaway, Phys. Rev. A **34**, 130 (1986).

[24] J. F. Williams, *Progress in Atomic Spectroscopy,* edited by W. Hanle and H. Kleinpoppen (Plenum, New York, 1979), Part B, p. 1031.